Aluminum(III) Interactions with the Acid Derivative Amino Acid Chains

Jose M. Mercero, Joseph E. Fowler, and Jesus M. Ugalde*

Kimika Fakultatea, Euskal Herriko Unibertsitatea, P.K. 1072, 20080 Donostia, Euskadi, Spain

Received: July 15, 1999; In Final Form: February 23, 2000

Aluminum(III) and magnesium(II) interactions with the asparagine and glutamine amino acid chains are studied by the density functional approach. Bader analysis and natural bonding orbital analysis were also performed to analyze the bonding interactions. We began by studying the interactions between the cations and the formamide, and we added two methyl groups sequentially to model more accurately the asparagine and the glutamine amino acid chains. The strongest binding energies for aluminum(III) and magnesium(II) are 372 and 140 kcal/mol, respectively, for asparagine chain and 404 and 145 kcal/mol, respectively, for the glutamine chain. The addition of the first methyl to the formamide has an important effect on the formamide−metal complexes, while the addition of the second methyl does not greatly change the properties of the complexes. The binding energies of these complexes are significantly smaller than those of the aluminum(III)/magnesium-(II) interactions with the acidic amino acid chains.

I. Introduction

The aluminum(III) cation has gained interest significantly in the scientific world over the last few years[1] after many negative aspects involving its effects in biological systems were reported. Many of these works concern how the aluminum(III) cation may enter the organism[2,3] and then deposit in different parts of the organism (principly in the brain[4] and bones[5]) and finally the mechanism by which it enters the cell.[3]

One of the principal thrusts of investigation regarding aluminum(III) toxicity has been focused on its possible role in Alzheimer disease development, although the direct link with this disease is still controversial.[6] The toxic effects of the aluminum(III) cation result from its competition with other essential metal cations such as magnesium(II), calcium(II), zinc-(II), or iron(III). Additionally, magnesium(II) has been shown to be one of the most affected cations by aluminum(III) interference.[7] The magnesium(II) cation is the simplest metal that competes with aluminum(III), both having similar sizes, which is a dominant factor over the charge identity concerning metal ion competition.[8,9] Previously we investigated the interaction between aluminum(III) and acidic amino acid chains, and compared our results to equal levels of theory applied to magnesium(II).[10]

A few works can be found in the literature where the interactions between cations and amino acids are studied using ab initio methods,[11−14] but all of these works are focused on divalent cations. In this work, we study the interactions between the aluminum(III) cation and acid derivative aminoacid chains, in the gas phase, to provide insight into the binding of these complexes because it will present a good model of more complicated biochemical systems, and provide some solid foundations which could help to devise reliable strategies for the modeling of biomolecules interacting with metal cations.

Solvent effects are important. However, to learn more about how the solvent affects the interaction between aluminum(III) and amino acids, it is necessary first to understand the bare system. In this context the present research expands our previous work on acidic amino acid chains and provides more insight into these specific interactions of aluminum(III). Naturally, an obvious extension of these studies is to properly include the solvent, recalculate the interaction, and compare with the bare system to extract information on the effects of the solvent. This will set the investigation of the solvation on firm grounds.

Formamide is a bidentate base which permits metal interactions with either N or O or both N and O in a bidentate orientation. It is also the simplest model for the peptidic bond, and the functional group of asparagine and glutamine amino acids. Formamide protonation has also been used to achieve a better understanding of proton exchange in proteins[15] and hydrolysis of the peptide bond.[16] Recently, different monocation interactions with formamide Li^+, Na^+, Mg^+, Al^+,[17,18] and Cu^+ [19]) have been investigated. Some studies concerning metal cation−asparagine and glutamine amino acid interactions are present in the literature.[20,21] In these experimental studies, since the amino acid is studied, the metal cation tends to interact with the acid part of the amino acid.

Recent advances[22] in the experimental accessibility of multiply charged cation, and in particular triply charged cations, make the present study very timely to rationalize the mechanism of interactions of aluminum(III) with biological systems. As wisely indicated by Schröder and Schwarz in a recent Feature Article in the Journal, "Nevertheless, some implications derived from fundamental studies of small, multiply charged ions... are of crucial importance for the understanding of the behavior of large molecules".

In the present work, first, we study the interactions between both aluminum(III) and magnesium(II) cations and the smallest functional moiety of the asparagine and glutamine amino acids: the formamide. Then, we introduce a methyl group to describe more accurately the asparagine. Afterward a second methyl was added to represent the glutamine amino acid chain.

II. Methods

All calculations were carried out with the GAUSSIAN98[23] package. Density functional methods have proven to give excellent results in most chemical systems,[24] with results comparable to those given by CPU-intensive electron-correlation methods. However, it frequently overestimates bond dissociation

10.1021/jp992415g CCC: $19.00
Published on Web 07/11/2000

TABLE 1: Energies of the Minimum Structures (*E*, hartrees) and Binding Energies of the Metal Complexes (BE, kcal/mol) for the Formamide and Its Tautomer 2 (Y = H) and for the Methyl and Ethyl Derivatives (Y = CH_3 and CH_2CH_3, Respectively)[a]

		Y = H		Y = CH_3			Y = CH_2CH_3		
	X	*E*	BE	*E*	R	BE	*E*	R	BE
xo1		−33.308 816		−40.149 018	a		−46.979 219	f	
	Al	−274.210 239	322.57	−281.101 549	c	354.64	−287.988 134	c	390.02
	Mg	−232.734 364	124.30	−239.589 201	a	133.48	−246.436 763	g	144.37
xbts1		−33.282 097		−40.126 043	c		−46.957 389	g	
	Al	−274.185 710	307.18	−281.100 568	a	354.03	−287.968 086	f	377.44
	Mg	−232.702 399	104.24	−239.573 128	c	123.39	−246.411 914	g	128.75
xn2.1		−33.288 405		−40.128 983	a		−46.959 316	a	
	Al	−274.163 782	306.23	−281.064 823	a	344.17	−287.955 643	e	382.13
	Mg	−232.685 064	106.17	−239.544 621	a	118.08	−246.381 391	a	122.12
xo2.1	Mg	−232.650 785	84.66						
xb2.2		−33.279 442		−40.117 867	a		−46.948 526	a	
	Al	−274.204 631	331.86	−281.109 884	a	372.45	−287.973 111	b	393.09
	Mg	−232.715 685	125.38	−239.580 465	a	140.57	−246.418 621	a	145.48
xn2.3		−33.282 868		−40.123 260	a		−46.953 960	a	
	Al	−274.180 680	316.83	−281.065 240	a	344.38	−287.991 130	a	404.39
	Mg	−232.700 872	111.25	−239.556 382	a	125.46	−246.412 286	a	141.50
xn2.4		−33.282 842		−40.124 310	a		−46.954 560	a	
	Al	−274.170 397	310.38	−281.072 672	a	349.09	−287.990 693	a	404.12
	Mg	−232.693 168	111.25	−239.551 217	a	122.22	−246.410 793	a	140.57
Al		−240.387 372							
Mg		−199.227 471							

[a] R indicates the conformation of the rotamer.

energies.[25] The hybrids of HF and DFT theories increment the accuracy of the dissociation energy as was validated by Johnson et al.[25] The Becke proposed hybrid[27] (B3), combined with the correlation functionals reported by Lee, Yang, and Parr[28] (LYP), has been chosen for this work.

An all-electron 6-31G split valence basis set was used for each metal, and the set of relativistic compact effective core potentials of Stevens et al.[29] was used with their corresponding 31 split valence basis sets for all other atoms. The basis set for each atom was augmented with a diffuse sp set of functions and a polarization set of p- and d-functions. We shall refer to this basis as DZ+(d). Frequencies were calculated at this level of theory and the corresponding zero-point vibrational energy (ZPVE) corrections made to the total energy. The binding energy was evaluated with the ZPVE-corrected energies as follows:

$$B_e = (E_l + E_x) - (E_{xl}) \quad (1)$$

where "xl" is for the complex, and "x" for the metal cation, and "l" for the ligand.

To analyze the interactions of the cation with the formamide residues, Bader analysis[30] was performed with the AIMPAC[31] package. Also natural bond order analysis was used to investigate natural charges.[32]

The MOLDEN, visualization of molecular and electronic structure, program[33] was used for making the figures.

III. Results and Discussion

We have studied the interactions of the aluminum(III) and magnesium(II) cations with the asparagine and glutamine amino acid chains. First, we focused on the interactions of the cation with the smallest representation of the functional group, the formamide. We have also considered one of the two tautomers of the formamide (**2** in Figure 1). We have not studied in detail the second tautomer (**3** in Figure 1) because of its high relative energy and its radicaloid character.[17] Then we added methyl groups to obtain a more realistic representation of the amino acids. The following example should make clear the notation used in this work. The notation **xn2.1** indicates that a metal atom is present (**x**), and bound to the nitrogen atom **n** (note that a **b** will be used to indicate bidentate bonding), in a structure most directly related to the structure **2.1**.

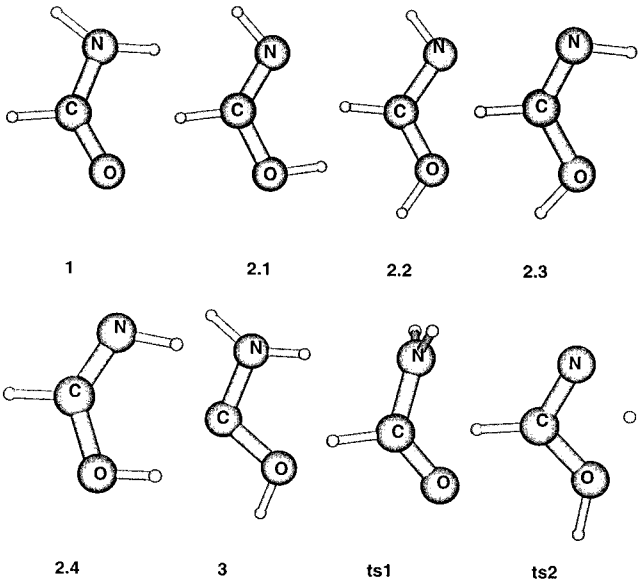

Figure 1. Formamide **1** and **ts1** with its tautomers **2.n** and **3**.

A. X−HCONH$_2$ Complexes. Using the B3LYP method and the basis set described above, two different C_s isomers have been located for the formamide, a planar structure (**1** in Figure 1) and a transition state with an imaginary frequency which corresponds to the rotation of the NH_2 (**ts1**). Two tautomers are known for the formamide (see **2.n** and **3** in Figure 1). However, as stated above, only the rotamers of tautomer **2** have been studied in this work. All four rotamers of **2** present C_s symmetry. A transition state was also found which connects the formamide and the tautomer **ts2**, with an imaginary frequency corresponding to the passing of the hydrogen atom from the nitrogen to the oxygen.

The formamide structure **1** is the most stable of all the studied structures (see Table 1), and the rotation barrier of the NH_2 is 16.77 kcal/mol. Structure **2.1** is 12.81 kcal/mol higher in energy and is the global minimum of the tautomer. The other three tautomer **2** rotamers are around 5 kcal/mol higher in energy. Recall that Tortajada et al.[17] reported an energy difference between **1** and **2.1** of 11.50 and 11.40 kcal/mol at the G2 and G2(MP2) levels of theory, respectively. Finally, **ts2** lies 43.50 kcal/mol above structure **1**, which agrees well with the values

TABLE 2: Geometrical Features of the Formamide and Its Tautomer 2 Complexes (Y = H) and the Corresponding Methyl and Ethyl Derivatives (Y = CH_3 and CH_2CH_3, Respectively)[a]

		Y = H					Y = CH_3							Y = CH_2CH_3						
	X	X−O	X−N	C−O	C−N	OCN	X−O	X−N	C−O	C−N	C−C	OCN	R	X−O	X−N	C−O	C−N	C−C	OCN	R
xo1				1.229	1.376	124.8			1.234	1.382	1.538	122	a			1.234	1.383	1.543	121.74	f
	Al	1.711		1.371	1.306	118.2	1.747		1.383	1.290	1.533	125.7	c	1.785		1.341	1.299	1.569	125.11	c
	Mg	1.820		1.300	1.311	122.7	1.803		1.319	1.319	1.510	118.6	a	1.871		1.299	1.320	1.538	119.51	g
xbts1				1.219	1.457	125.4			1.224	1.407	1.533	122.7	c			1.224	1.470	1.528	122.88	g
	Al	1.855	2.024	1.257	1.500	110.2	1.800	1.980	1.292	1.542	1.471	106.3	a	1.862	2.048	1.270	1.506	1.532	108.86	f
	Mg	2.035	2.182	1.237	1.472	113.6	1.994	2.150	1.252	1.501	1.493	110.8	c	1.989	2.139	1.253	1.507	1.497	110.52	g
xn2.1				1.360	1.282	121.9			1.370	1.286	1.523	119.2	a			1.372	1.285	1.529	119.07	a
	Al		1.856	1.240	1.403	135.3		1.957	1.257	1.391	1.562	131.8			1.993	1.274	1.347	1.607	130.77	e
	Mg		1.987	1.295	1.335	128.8		1.973	1.310	1.346	1.510	124.1	a		1.966	1.312	1.344	1.519	124.19	a
xo2.1	Mg	1.920		1.570	1.230	111.4														
xb2.2				1.370	1.278	119.7			1.379	1.282	1.534	117	a			1.379	1.281	1.540	116.81	a
	Al	1.907	1.879	1.408	1.300	107.1	1.853	1.845	1.468	1.321	1.485	102.7	a	1.927	1.886	1.426	1.310	1.548	103.98	b
	Mg	2.150	2.040	1.380	1.290	110.8	2.098	2.013	1.407	1.299	1.501	107.7	a	2.085	2.008	1.412	1.299	1.506	107.6	a
xn2.3				1.381	1.275	124.5			1.389	1.280	1.524	121.7	a			1.390	1.280	1.529	121.52	a
	Al		1.839	1.258	1.414	112.6		1.842	1.277	1.449	1.492	106.7	a		1.785	1.274	1.366	1.544	116.7	a
	Mg		1.954	1.299	1.328	118.8		1.955	1.312	1.338	1.512	115	a		1.962	1.313	1.322	1.529	117.93	a
xn2.4				1.375	1.281	129.8			1.385	1.285	1.518	126.9	a			1.386	1.284	1.523	126.72	a
	Al		1.836	1.255	1.408	122.5		1.793	1.268	1.372	1.545	128.8	a		1.797	1.274	1.366	1.540	127.09	a
	Mg		1.982	1.295	1.334	127.5		1.963	1.307	1.338	1.511	124.6	a		1.973	1.311	1.326	1.526	126.22	a

[a] R indicates the conformation of the rotamer.

of 46.6 and 45.9 kcal/mol at the G2 and G2(MP2) levels of theory, respectively, reported by Tortajada et al.

The geometries of these $HCONH_2$ species are shown in Table 2. We focus our attention on the atoms which will be involved in the metal binding. The geometric features of the formamide and its NH_2 rotation transition state are very similar, with the only remarkable difference being in the C−N bond, which measures 1.457 Å in the transition-state structure and 1.376 Å in the formamide ground state. As can be seen, the effect of "turning off" the C−N π interaction is significant. Similarly, the geometries of the tautomer and its rotamers are nearly identical (except, of course, for the rotations).

The formamide and its tautomer present different binding possibilities, monodentate binding to the oxygen in the formamide (**xo1**, **xots1**), and to either the oxygen (**xo2.1**, **xo2.3**, **xo2.4**) or nitrogen (**xn2.1**, **xn2.3**, **xn2.4**) of the tautomer. Bidentate binding is also possible in both compounds (**xbts1**, **xb2.2**).

The aluminum−formamide interaction presented only oxygen monodentate **Alo1** and bidentate binding **Albts1** possibilities (note that **Alots1** is a transition state). The B3LYP/DZ+(d) wavefunction for the **Alo1** isomer in C_s symmetry experiences RHF-UHF instability. We have located a C_1 complex where the aluminum is out of the NCO plane by 47°, which is a stable minimum. The formamide−tautomer **2.n** aluminum(III) binding, however, presented Al−N monodentate (**Aln2.1**, **Aln2.3**, and **Aln2.4**) and bidentate **Alb2.2** bindings. All of these complexes have C_s symmetry, except the **Aln2.3** structure which has C_1 symmetry with the aluminum 17° out of the NCO plane.

The geometric parameters of these complexes are shown in Table 2. Among the aluminum complexes, in the oxygen monodentate complex, logically, we observe that the C−O bond is elongated, while the C−N bond shrinks, similarly, the opposite effect is detected in the nitrogen-binding aluminum complexes. The Al−O bond in **Alo1** measures 1.711 Å, and the C−O bond is 0.14 Å longer and the C−N bond 0.07 Å shorter than in **1**. In the nitrogen−metal monodentate binding complexes, the shortest Al−N bond is found in the **Aln2.4** complex, with a value of 1.836 Å, while this bond has a length of 1.856 Å in **Aln2.1**. In the bidentate binding modes, X−O and X−N bond lengths are 1.907 and 1.879 Å, respectively, in **Alb2.2** and 1.855 and 2.024 Å, respectively, in **Albts1**. The C−O bond elongates by 0.038 Å in both complexes, while the C−N bond shrinks by 0.043 and 0.022 Å in **Albts1** and **Alb2.2**, respectively. Looking at the ligand after binding to the aluminum, we see that both bidentate modes alter the geometry less than the monodentate modes.

Structurally related magnesium(II) complexes were also located in our B3LYP/DZ+(d) having C_s symmetry. A **Mgots1** structure was not found; instead **Mgo1.1** was present. All of these complexes have C_s symmetry. The geometrical features of these compounds are shown in Table 2; as expected, various signals of weaker bonding in the magnesium complexes are observed, e.g., longer metal−ligand bond lengths and smaller effects of complexation suffered by the ligand.

Analyzing the natural charge distribution of the complexes, we also observe that the charge transfer is larger at the aluminum complexes. While the aluminum gains −0.52 e^- upon complexation, magnesium only receives a transfer of −0.05 e^- in the **Xo1** complexes. The charge transfer to the aluminum atom in the bidentate complex is very similar to that seen in the monodentate **Alo1** complex, but the **Mgb2.2** complex demonstrates a charge transfer almost 3 times greater than that seen in the corresponding monodentate complex. These charge transfers are slightly smaller than those found earlier for the bidentate $X-COO]^{2+}$ complexes.[10] In these complexes, a charge of −0.651 e^- was transferred to aluminum and −0.233 e^- to magnesium.

In the aluminum(III) complexes, the most stable binding occurs in the **Alb2.2** complex, with a binding energy of 331.86 kcal/mol, while the monodentate oxygen and nitrogen (the strongest, **Aln2.3**) binding energies are 322.57 and 316.83 kcal/mol, respectively. Recall that we are comparing the binding energies with respect to two different ligands, the formamide and its tautomers. In the magnesium complexes, the tightest bond occurs also in the **Mgb2.2** complex, where the binding energy is 125.38 kcal/mol but is only 1 kcal/mol stronger than the bonding found in the **Mgo1** structure. Finally, the **Mgo2.1** complex, namely, the only monodentate metal−oxygen binding minimum on the tautomer surface, has a binding energy of only 84.66 kcal/mol.

Comparing these binding energies with those in the $X-CO-OH]^{+/2+}$ complexes,[10] the binding energies here are much smaller. Aluminum and magnesium had bidentate binding energies of 710.21 and 364.37 kcal/mol, respectively, in the $X-COOH]^{2+/3+}$ complexes, which are more than twice the binding energies of the $X-ONH_2CH]^{2+/3+}$ complexes. This binding energy difference is largely due to the negative charge of the $HCOO^-$ ligand. The monodentate $Al-OCOH]^{2+}$ binding

TABLE 3: NBO Natural Charges of the Formamide Complexes and the Corresponding Methyl Derivatives[a]

		Y = H							Y = CH_3									
	X	X	O	N	H_n	$H_{n/o}$	C	H_c	X	O	N	H_n	$H_{n/o}$	C_1	C_2	$H_{in\ plane}$	H_1	H_2
xo1			−0.657	−0.877	0.405	0.413	0.596	0.120		−0.678	−0.878	0.404	.415	0.750	−0.679	0.197	0.233	0.233
	Al	2.479	−0.981	−0.524	0.542	0.520	0.658	0.304	2.352	−1.008	−0.650	0.470	0.454	0.822	−0.589	0.265	0.269	0.269
	Mg	1.953	−1.064	−0.713	0.477	0.463	0.659	0.224	1.951	−1.098	−0.728	0.528	0.501	0.826	−0.679	0.360	0.366	0.366
xbts1			−0.577	−0.978	0.397	0.397	0.629	0.132		−0.604	−0.975	0.396	0.396	0.782	−0.690	0.227	0.235	0.235
	Al	2.428	−0.638	−1.084	0.569	0.569	0.766	.389	2.391	−0.722	−1.077	0.551	0.551	0.889	−0.713	0.332	0.399	0.399
	Mg	1.848	−0.668	−1.113	0.488	0.488	0.692	0.265	1.838	−0.729	−1.108	0.477	0.477	0.853	−0.717	0.272	0.317	0.317
xn2.1			−0.736	−0.781	0.368	0.506	0.487	0.157		−0.750	−0.784	0.364	0.509	0.653	−0.667	0.214	0.230	0.230
	Al	2.379	−0.483	−1.175	0.531	0.641	0.734	0.372	2.043	−0.533	−1.020	0.513	0.611	0.874	−0.547	0.323	0.365	0.370
	Mg	1.878	−0.598	−1.178	0.451	0.538	0.657	0.252	1.859	−0.625	−1.190	0.443	0.525	0.825	−0.677	0.248	0.295	0.295
xo2.1	Mg	1.890	−1.066	−0.564	0.471	0.583	0.457	0.230										
xb2.2			−0.730	−0.727	0.362	0.497	0.464	0.133		−0.733	−0.727	0.357	0.493	0.631	−0.684	0.222	0.220	0.220
	Al	2.483	−0.874	−9.440	0.577	0.692	0.680	0.378	2.443	−0.910	−0.987	0.561	0.673	0.843	−0.693	0.345	0.363	0.363
	Mg	1.865	−0.847	0.960	0.483	0.607	0.580	0.272	1.854	−0.873	−0.982	0.474	0.597	0.757	−0.697	0.287	0.292	0.292
xn2.3			−0.755	−0.722	0.361	0.499	0.464	0.152		−0.761	−0.735	0.343	0.491	0.632	−0.669	0.203	0.214	0.214
	Al	2.524	−0.512	−1.230	0.535	0.652	0.737	0.290	2.332	−0.528	−1.102	0.525	0.606	0.879	−0.718	0.492	0.347	0.347
	Mg	1.890	−0.627	−1.153	0.454	0.577	0.641	0.216	1.854	−0.639	−1.160	0.442	0.551	0.802	−0.681	0.337	0.198	0.198
xn2.4			−0.740	−0.740	0.341	0.491	0.480	0.172		−0.755	−0.756	0.341	0.492	0.648	−0.652	0.231	0.224	0.224
	Al	2.455	−0.457	−1.191	0.525	0.638	0.734	0.296	2.387	−0.523	−1.114	0.540	0.624	0.806	−0.493	0.024	0.375	0.375
	Mg	1.886	−0.596	−1.160	0.439	0.557	0.649	0.226	1.869	−0.625	−1.151	0.440	0.552	0.800	−0.661	0.171	0.302	0.302

[a] Note that the hydrogens are bound to the non-hydrogen atom to its left in the table. The subscript n/o indicates the hydrogen bound to N in **1** and O in the tautomers. $H_{in-plane}$ is the hydrogen which lies in the CCH symmetry plane. H_1 is the hydrogen which is on the metal cation side when there is no C_s symmetry. Finally the carbon numbers are in positional order counting from the carbon to the oxygen and nitrogen atoms.

energy is also significantly larger than the energy of the monodentate binding to the formamide, around 350 kcal/mol larger.

Previous calculations concerning magnesium(II) cation and formamide were performed by Garmer and Gresh,[11] but they only focused on the formamide ground state, i.e., our **Mgo1** complex. They report a Mg−O bond length of 1.80 Å at the HF level of theory using a 6-631G(2d) basis set for the magnesium,[34] and a SBK-31(2d) set for the ligand atoms. Their binding energy of 121.1 kcal/mol at the MP2//HF level of theory compares well with our value of 124.30 kcal/mol.

The X−O bonding leads to a charge transfer occurring from the ligand to the metal cation. To garner a better understanding of this process, we have performed Bader's topological analysis, and observed that the metal cation activates the C−O bond; hence, the oxygen atom gains negative charge by depopulating the C═O bond. Let us look at **Mgo1** to illustrate the point. Upon metal binding, the energy density of the C−O bond critical point becomes less negative (changes from −0.635 to −0.526; see Table 4) and the bond length elongates (about 0.070 Å). The energy density of the C−N bond critical point becomes more negative (around 0.05 in our example), and the C−N bond shrinks. Observe that this applies to either Al or Mg X−O bindings. Similarly, the bonding of the metal to the nitrogen causes the C−N energy density to become less negative and the C−O energy density to become more negative. In the bidentate bonding modes, both C−O and C−N bonds are activated after the metal binding (the energy densities are lower after the metal binding), so that the bonds are longer than in the uncomplexed ligands (see Tables 2 and 4).

Finally, we mention another difference between the aluminum(III) and magnesium(II) complexes. According to the Bader analysis, it is easy to discriminate between covalent and ionic bonds. When the energy density at the bond critical point is larger than zero, the bond can be classified as an ionic bond, while if it is less than zero then the bond is considered covalent.[30] The Yañez[17] group in their aluminum(I) and magnesium(I) formamide study reported electrostatic interactions between aluminum(I) and formamide, and in the **xb2.2** complex, they only located bond critical points between the cation and the nitrogen atom but not with the oxygen. In our study, as is shown in Table 4, we see that, for aluminum(III) ligand binding, all but the **Alo1** and the Al−O bond in **Alb2.2** are covalent bonds, while all of the magnesium(II) bonds are reported as ionic in the Bader analysis. Comparing the formamide and aluminum(I) and magnesium(I) interactions,[17] the structure analogous to **xo1** was found to bind most tightly for both monocations, both of them having similar binding energies around 48 kcal/mol (significantly lower than in our case). They found **xb2.2** complex binding to be only 3 kcal/mol lower in energy for magnesium(I) and 7 kcal/mol lower in energy for aluminum(I). In terms of cation−ligand bonding, in the **xb2.2** complex, they located bond critical points only between the cation and the nitrogen atom; no critical point existed between the metal and the oxygen.[17]

B. X−CH_3CONH_2 Complexes. To represent more realistically the asparagine chain, a methyl group was added to the formamide and its tautomer. Thus, due to the rotation of the methyl group, we have located three stationary points for each of the previously described isomers. These three new isomers correspond to the rotation of the CH_3 group around the C−C bond. In redefining the previously described nomenclature to include these new isomers, we will just add an **M** for methyl derivative at the beginning, and **a**, **b**, or **c** at the end corresponding to the methyl rotation; e.g., for the **xn2.1** tautomer isomer, when the N is eclipsed with one of the hydrogen atoms of the methyl group, the label will be **M-xn2.1a**, when the OCN plane is perpendicular to one of the C−H planes, it will be **M-xn2.1b**, and finally, when the oxygen atom is eclipsed with one of the methyl hydrogens, we will refer to the isomer as **M-xn2.1c**. As can be observed, the number of stationary points for the species of interest has augmented significantly. However, these three rotamers generally serve to demonstrate the free rotor character of the methyl group, and the geometric and energetic properties of each of the CH_3 rotamers is nearly degenerate. Thus, we will only discuss the most stable structures of the corresponding series.

The methylformamide **M-1a** is the lowest energy rotamer, and both energetically degenerate rotamers **M-1b** and **M-1c** have a negative frequency corresponding to the rotation of the methyl group. In the CH_3CONH_2 case the NH_2 rotation barrier is 14.42 kcal/mol, slightly lower than in the formamide case.

In the methylformamide tautomer derivatives, the methyl group again is more or less a free rotor. The **a** orientation of the methyl group is preferred, presenting slightly lower energies than the other two rotamers. The **M-2.1a** case is the most stable

TABLE 4: Bader Analysis Results for the Formamide/Tautomer Complexes: Charge Densities (Y = H), and Methyl and Ethyl Derivatives (Y = Methyl and Y = Ethyl, Respectively), Laplacian of the Charge Densities ($\nabla^2\rho$), and Energy Densities ($H(r)$) of the Corresponding Bond Critical Points

			Y = H				Y = CH_3						Y = CH_2CH_3					
	X		CO	CN	XO	XN	CO	CN	CC	XO	XN	XH	CO	CN	CC	XO	XN	XC
xo1		ρ	0.371	0.343			0.398	0.310	0.246				0.397	0.309	0.246			
		$\nabla^2\rho$	−1.056	−1.056			−0.143	−0.986	−0.579				−0.128	−0.980	−0.574			
		$H(r)$	−0.635	−0.569			−0.687	−0.357	−0.199				−0.684	−0.465	−0.198			
	Al	ρ	0.267	0.368	0.095		0.243	0.378	0.238	0.095			0.293	0.371	0.221	0.078		
		$\nabla^2\rho$	−0.228	−1.057	0.799		−0.336	−1.074	−0.553	0.804			−0.297	−1.065	−0.462	0.573		
		$H(r)$	−0.400	−0.635	0.006		−0.341	−0.656	−0.218	0.007			−0.454	−0.639	−0.175	0.005		
	Mg	ρ	0.327	0.362	0.064		0.316	0.357	0.255	0.064			0.338	0.356	0.247	0.624		
		$\nabla^2\rho$	−0.216	−1.014	0.621		−0.269	−1.055	−0.636	0.661			−0.345	−1.073	−0.582	0.540		
		$H(r)$	−0.526	−0.619	0.023		−0.504	−0.605	−0.229	0.023			−0.554	−0.600	−0.203	0.018		
xbts1		ρ	0.397	0.322			0.402	0.276	0.249				0.401	0.276	0.253			
		$\nabla^2\rho$	0.107	−1.170			0.127	−0.765	−0.591				0.141	−0.765	−0.604			
		$H(r)$	−0.675	−0.469			−0.686	−0.286	−0.204				−0.684	−0.287	−0.210			
	Al	ρ	0.374	0.259	0.076	0.064	0.348	0.235	0.252	0.085	0.068		0.358	0.252	0.220	0.077	0.060	
		$\nabla^2\rho$	−0.083	−0.678	0.463	0.227	−0.324	−0.536	−0.630	0.594	0.284		−0.158	−0.636	−0.447	0.480	0.221	
		$H(r)$	−0.631	−0.256	−0.003	−0.013	−0.580	−0.214	−0.286	−0.001	−0.011		−0.598	−0.246	−0.205	−0.002	−0.011	
	Mg	ρ	0.390	0.274	0.043	0.362	0.378	0.260	0.256	0.048	0.039		0.377	0.254	0.255	0.048	0.039	
		$\nabla^2\rho$	0.048	−0.775	0.296	0.196	−0.106	−0.681	−0.644	0.348	0.220		−0.085	−0.645	−0.638	0.354	0.228	
		$H(r)$	−0.662	−0.290	0.009	0.005	−0.641	−0.259	−0.245	0.077	0.006		−0.636	−0.249	−0.247	0.011	0.006	
xn2.1		ρ	0.294	0.391			0.290	0.390	0.250				0.288	0.389	0.250			
		$\nabla^2\rho$	−0.433	−1.144			−0.480	−1.190	−0.610				−0.478	−1.170	−0.595			
		$H(r)$	−0.460	−0.684			−0.450	−0.678	−0.223				−0.445	−0.678	−0.206			
	Al	ρ	0.369	0.287		0.084	0.360	0.300	0.210		0.070		0.353	0.329	0.200		0.064	
		$\nabla^2\rho$	0.174	−0.872		0.407	−0.070	−0.920	−0.430		0.250		−0.175	−1.047	−0.367		0.227	
		$H(r)$	−0.605	−0.376		−0.014	−0.608	−0.400	−0.178		−0.018		−0.582	−0.509	−0.148		−0.012	
	Mg	ρ	0.337	0.345		0.054	0.330	0.340	0.250		0.060		0.326	0.339	0.249		0.057	
		$\nabla^2\rho$	−0.220	−1.151		0.368	−0.300	−1.160	−0.630		0.380		−0.302	−1.141	−0.605		0.392	
		$H(r)$	−0.550	−0.559		0.010	−0.535	−0.530	−0.228		0.005		−0.528	−0.540	−0.227		0.010	
xo2.1	Mg	ρ	0.172	0.425	0.054													
		$\nabla^2\rho$	−0.154	−0.706	0.432													
		$H(r)$	−0.146	−0.768	0.015													
xb2.2		ρ	0.287	0.395			0.283	0.393	0.247				0.282	0.393	0.246			
		$\nabla^2\rho$	−0.459	−1.124			−0.494	−1.176	−0.574				−0.488	−1.157	−0.561			
		$H(r)$	−0.442	−0.696			−0.431	−0.689	−0.201				−0.429	−0.689	−0.197			
	Al	ρ	0.258	0.375	0.062	0.082	0.226	0.361	0.244	0.069	0.087		0.248	0.367	0.216	0.058	0.079	
		$\nabla^2\rho$	0.431	−1.112	0.365	0.420	−0.442	−1.202	−0.589	0.466	0.485		−0.447	−1.137	−0.428	0.335	0.418	
		$H(r)$	−0.164	−0.648	0.000	−0.012	−0.287	−0.607	−0.271	0.004	−0.011		−0.350	−0.628	−0.193	0.000	−0.010	
	Mg	ρ	0.277	0.386	0.029	0.048	0.261	0.380	0.252	0.033	0.051		0.257	0.379	0.250	0.034	0.051	
		$\nabla^2\rho$	0.392	−1.138	0.178	0.318	−0.440	−1.211	−0.628	0.220	0.343		−0.435	−1.191	−0.612	0.232	0.348	
		$H(r)$	0.324	−0.676	0.006	0.009	−0.381	−0.655	−0.238	0.008	0.010		−0.373	−0.655	−0.236	0.008	0.009	
xn2.3		ρ	0.279	0.395			0.275	0.393	0.252				0.274	0.393	0.251			
		$\nabla^2\rho$	−0.451	−1.109			−0.481	−1.157	−0.608				−0.475	−1.144	−0.601			
		$H(r)$	−0.421	−0.698			−0.410	−0.691	−0.209		0.000		−0.409	−0.691	−0.207			
	Al	ρ	0.374	0.287		0.094	0.337	0.271	0.254		0.087		0.357	0.328	0.243		0.099	0.060
		$\nabla^2\rho$	−0.037	−0.932		0.525	−0.206	−0.812	−0.643		0.447		−0.211	−1.152	−0.563		0.634	0.197
		$H(r)$	−0.627	−0.384		−0.015	−0.644	−0.325	−0.257		−0.012		−0.594	−0.496	−0.199		−0.012	−0.015
	Mg	ρ	0.568	0.511		0.001	0.338	0.354	0.289		0.057		0.329	0.361	0.250		0.058	
		$\nabla^2\rho$	4.333	1.878		0.004	−0.282	−1.198	−0.818		0.392		−0.363	−1.232	−0.599		0.414	
		$H(r)$	−0.861	−0.763		0.001	−0.554	−0.581	−0.287		0.015		−0.534	−0.597	−0.210		0.011	
xn2.4		ρ	0.282	0.389			0.278	0.388	0.255				0.277	0.388	0.254			
		$\nabla^2\rho$	−0.436	−1.120			−0.474	−1.152	−0.630				−0.472	−1.135	−0.620			
		$H(r)$	−0.443	−0.683			−0.418	−0.675	−0.216				−0.415	−0.676	−0.213			
	Al	ρ	0.360	0.289		0.088	0.361	0.323	0.248		0.097	0.049	0.355	0.326	0.246		0.097	0.062
		$\nabla^2\rho$	0.046	−0.921		0.459	−0.198	−1.103	−0.598		0.607	0.090	−1.198	−1.117	−0.585		0.603	0.213
		$H(r)$	−0.592	−0.388		−0.014	−0.602	−0.462	−0.201		−0.012	−0.015	−0.839	−0.488	−0.205		−0.011	−0.016
	Mg	ρ	0.339	0.347		0.056	0.332	0.346	0.258		0.058		0.338	0.356	0.247		0.062	
		$\nabla^2\rho$	−0.239	−1.166		0.381	−0.324	−1.189	−0.648		0.408		−0.345	−1.073	−0.582		0.540	
		$H(r)$	−0.553	−0.563		0.086	−0.540	−0.553	−0.227		0.010		−0.554	−0.600	−0.203		0.018	

on the tautomer potential surface, and **M-2.4a**, **M-2.3a**, and **M-2.2a** are 2.93, 3.59, and 6.98 kcal/mol higher in energy, respectively, at the employed level of theory.

Table 2 includes the geometric features of the most stable rotamers (note that the Cartesian coordinates of all the species are available upon request). The alteration of the geometric features due the inclusion of the methyl group is almost insignificant. Upon the inclusion of the methyl group, both oxygen and nitrogen atoms gain slightly in negative charge, due to the electron donor property of the methyl group, while the carbon bound to these atoms increases in positive charge. (See Table 3 for more details.)

With the addition of the aluminum(III) cation, complex types similar to those of the plain formamide ligand were encountered, plus the rotamers corresponding to the previously described methyl rotations. The geometrical parameters of these Al−methylformamide complexes are quite similar to those of the non-methylated complexes. In this case, however, compared with the formamide−aluminum complexes, important changes are observed with respect to energy.

The **M-Alo1c** and **M-Albts1a** structures are very close in energy, whereas the monodentate complex was more stable by about 15 kcal/mol in the non-methylated complex. In the methylformamide tautomer complexes, the **M-Alb2.2a** isomer is the most stable. Note that all of the **M-Aln2.1a** and **M-Aln2.3a** C_s symmetry species presented one imaginary frequency, corresponding to the breaking of the OCN plane. Thus, the most stable isomers of these conformations have C_1 symmetry, though the barrier to planarity is very small. The geometric parameters of these complexes are given in Table 2.

The magnesium interaction with these methyl derivatives follows the patterns observed in the earlier section with only slight variations in geometry as can be appreciated in Table 2. The methylformamide−magnesium interactions lead to the previously described complexes, **1** and **ts1**, with the corresponding methyl rotations **a**, **b**, and **c**. **M-Mgo1a** is the most stable

complex. The **M-Mgbts1b** and **M-Mgbts1c** structures are minima which lie about 10 kcal/mol higher in energy than **M-Mgo1a**; note that this difference has been reduced by about 10 kcal/mol compared with the magnesium−formamide complexes. The methylformamide tautomer−magnesium complexes also maintain properties similar to those in the previous section. Note that the **M-Mgo2.1** complex is not a stationary point on this potential surface, and no monodentate Mg−O binding complexes are found.

The electron-donor character of the methyl group strengthens the binding energy between the metal and the ligand. In the aluminum(III) complexes, the strongest binding occurs in the **M-Alb2.2a** complex, which has a binding energy of 372 kcal/mol. The other tautomer (**M-Aln2.1a**, **M-Aln2.3**, and **M-Aln2.4a**) complexes have binding energies around 345 kcal/mol. The **M-Alo1c** and **M-Albts1a** complexes have larger binding energies than the three monodentate tautomer rotamers. Both of these complexes have metal binding energies of 354 kcal/mol. When compared to the formamide case, these binding energies are stronger by 32 kcal/mol in the case of **M-Alo1a** and 47 kcal/mol in the case of **M-Albts1a**. The binding energy increase for the methyl tautomers lies between 28 kcal/mol in the **M-Aln2.3a** complex and 41 kcal/mol in the **M-Alb2.2a** complex. In the magnesium complexes, this increase in binding energy is smaller. The strongest binding is in the **M-Mgb2.2a** complex, at 140.57 kcal/mol, which is only 7 kcal/mol stronger than that of the **M-Mgo1a** complex. The binding energies for the **M-Mgn2.1a**, **M-Mgn2.3a**, and **M-Mgn2.4a** structures are 118.08, 125.46, and 122.22 kcal/mol, respectively. There is a binding energy increase after the inclusion of the methyl group in the ligand, by 12 kcal/mol in these complexes, which is significantly lower than the binding energy increase in the aluminum complexes. This behavior was also observed for the aluminum(III) and magnesium(II) interactions with the COO^- and CH_3COO^- ligands.[10] These binding energies are significantly lower than those of the aspartic acid amino acid chain with aluminum(III) and magnesium(II), which are 742 and 373 kcal/mol, respectively.

The charge transfer from the ligand to the metal is larger than in the non-methylated complexes, due to the methyl electron-donor character. This difference is remarkable in the **M-Aln2.1a** complex, where the aluminum gains in negative charge, changing from 2.379 to 2.043 e^-, which is even bigger that the charge transfer observed in the $Al\text{-}CH_3COO]^{2+}$ complex,[10] where the aluminum has a natural charge of $+2.295$ e^-, while in the other complexes this effect is smaller.

It is interesting to note that the bidentate complexes are those that experience the most stabilization yet, at least in the case of the aluminum complexes, the least change in natural charge upon the addition of the methyl to the formamide. The two bidentate Al−methylformamide complexes average 44 kcal/mol more binding energy than their non-methylated counterparts, while the monodentate complexes gain 34 kcal/mol on average. Nevertheless, Table 3 demonstrates that the natural charge on aluminum changes little in the two bidentate complexes between $Y = H$ and $Y = CH_3$.

The bonding explanation given by the Bader analysis in the previous section is extendable to the methylated cases. As can be observed in Table 4, there is not a significant change in the Bader topological analysis. The most remarkable fact is the Al−H covalent bond given by this procedure, in the **M-Aln2.4a** complex (shown in Figure 2), and the location of a ring critical point. The natural bonding orbital analysis revealed a three-center two-electron bond (3c,2e) formed among the Al−H−C atoms. However, this bond is not very strong, as the **M-Aln2.4a** complex is only 2 kcal/mol more stable than the **b** and **c** rotamers.

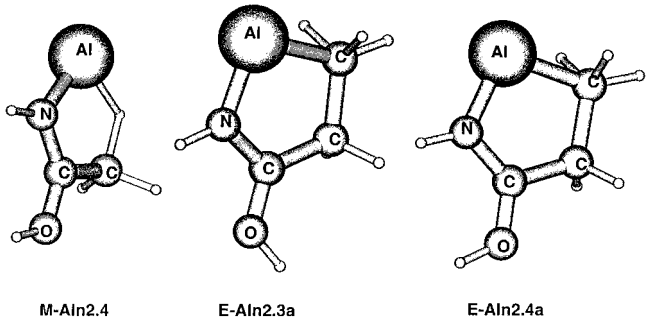

Figure 2. Structures **M-Aln2.4a**, **E-Aln2.3a**, and **E-Aln2.4a**, demonstrating the interaction between Al and the terminal unit.

CHART 1: Stationary Points Found for the Ethylformamide Rotamers, Each Rotation Corresponding to 30°

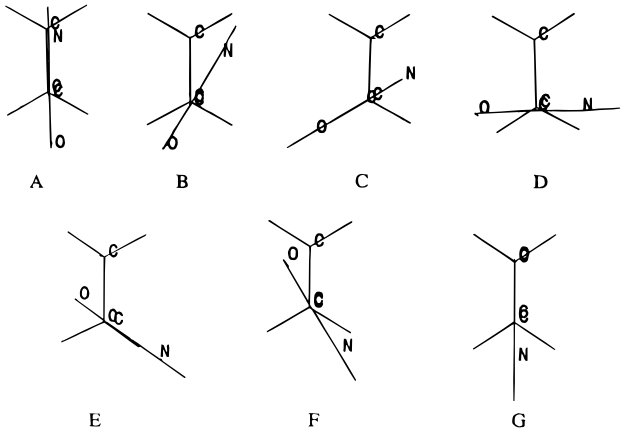

C. X−$CH_3CH_2CONH_2$ Complexes. Finally, to better describe the glutamine chain, we have added another methyl group to the CH_3CONH_2 ligand. Thus, due to the rotation capabilities of the ethyl group, a huge number of possible rotamers exist for ethylformamide and its tautomer derivatives. In this study seven isomers/rotamers of the isomers described in section 1 have been considered, all of them corresponding to the rotation of the NCO plane (rotation of the end-chain CH_3 group was also allowed, but details are not given here). Note that not all of these seven rotamers were stationary points in the corresponding potential energy surface. Similar to the nomenclature adopted previously, we denote these complexes with an **E** for ethyl at the beginning, and a letter at the end to differentiate the rotomers; e.g., **E-Aln2.1a** will correspond to the complex where the nitrogen atom is eclipsed with the terminal methyl carbon. The letters from **a** to **g** will imply dhNCCC dihedral angle rotations (i.e., NCO plane rotation around the C−C bond) of approximately 30°. These rotations are depicted in Chart 1.

For the $CH_3CH_2CONH_2$ **E-1** isomer, the **f** rotamer with a dhNCCC = 144.1° is the global minimum. Additionally **a**, **d**, and **e** rotamers were also found to be minima, all of them lying within an energetic range of 1 kcal/mol. Regarding the formamide tautomer ethyl derivatives, the ethyl derivative corresponding to the isomer **2.1** is the most stable, while **2.4**, **2.3**, and **2.2** are 3.0, 3.3, and 6.8 kcal/mol higher in energy (the **a** rotamer is the lowest in energy for each isomer). The geometric parameters analyzed in this work are nearly identical with those of the CH_3CONH_2, for both the formamide form and the tautomer. The same could be said for the natural charges of these ligands (see Table 5).

TABLE 5: NBO Natural Charges of the Ethylformamide Complexes[a]

	X	X	O	N	H_n	$H_{n/o}$	C_1	C_2	H_1	H_2	C_3	$H_{in\ plane}$	H_1	H_2
xo1			−0.679	−0.878	0.403	0.413	0.753	−0.479	0.199	0.226	−0.592	0.203	0.204	0.224
	Al	1.930	−0.942	−0.677	0.504	0.494	0.843	−0.453	0.341	0.384	−0.516	0.409	0.386	0.294
	Mg	1.882	−0.954	−0.737	0.462	0.467	0.791	−0.507	0.291	0.291	−0.700	0.329	0.193	0.193
xbts1			−0.605	−0.973	0.395	0.395	0.784	−0.491	0.232	0.232	−0.597	0.205	0.212	0.212
	Al	2.159	−0.683	−1.057	0.538	0.538	0.894	−0.479	0.327	0.378	−0.552	0.374	0.338	0.283
	Mg	1.833	−0.734	−1.110	0.475	0.475	0.852	−0.514	0.293	0.293	−0.603	0.263	0.238	0.238
xn2.1			−0.749	−0.786	0.507	0.364	0.657	−0.476	0.205	0.205	−0.606	0.216	0.230	0.230
	Al	1.791	−0.586	−1.034	0.492	0.594	0.867	−0.428	0.307	0.375	−0.500	0.417	0.390	0.315
	Mg	1.855	−0.629	−1.195	0.444	0.522	0.826	−0.487	0.291	0.291	−0.640	0.279	0.220	0.220
xb2.2			−0.734	−0.729	0.357	0.492	0.637	−0.489	0.218	0.218	−0.606	0.216	0.209	0.216
	Al	2.177	−0.866	−0.960	0.543	0.660	0.835	−0.479	0.340	0.340	−0.571	0.386	0.291	0.291
	Mg	1.850	−0.877	−0.990	0.470	0.595	0.761	−0.503	0.285	0.285	−0.613	0.272	0.231	0.231
xn2.3			−0.760	−0.743	0.364	0.496	0.637	−0.472	0.215	0.215	−0.591	0.203	0.218	0.218
	Al	2.341	−0.558	−1.123	0.538	0.612	0.843	−0.514	0.348	0.348	−1.001	0.484	0.341	0.341
	Mg	1.846	−0.646	−1.097	0.459	0.560	0.779	−0.511	0.293	0.293	−0.702	0.332	0.192	0.192
xn2.4			−0.754	−0.762	0.491	0.491	0.653	−0.460	0.225	0.225	−0.592	0.203	0.214	0.214
	Al	2.329	−0.547	−1.122	0.525	0.606	0.842	−0.509	0.357	0.357	−1.024	0.492	0.347	0.347
	Mg	1.841	−0.635	−1.105	0.442	0.551	0.785	−0.504	0.303	0.303	−0.717	0.327	0.198	0.198

[a] Note that the hydrogens are bound to the non-hydrogen atom to its left in the table. The subscript n/o indicates the hydrogen bound to N in **1** and O in the tautomers. $H_{in-plane}$ is the hydrogen which lies in the CCC symmetry plane. H_1 is the hydrogen which is on the metal cation side when there is no C_s symmetry. Finally the carbon numbers are in positional order counting from the carbon to the oxygen and nitrogen atoms.

After interaction with aluminum(III), the same number of rotamers have been analyzed. In most cases the formamide ethyl derivative−aluminum(III) complexes also show the free rotor character of the ethyl group. In the monodentate binding the **c** rotamer is the most stable (dhNCCC = 57.3°). Similar to the previous sections, the effect of the metal ligand binding to **E-ts1** in the bidentate orientation is that the imaginary frequency of the original ligand is lost, and for the **E-albts1** isomer the seven rotamers have been located, where **f** is the lowest energy rotamer and the other six lie within a range of 3 kcal/mol, **a**, **c**, **e**, and **g** being transition states.

The magnesium−ligand complexes present characteristics similar to those described in the previous sections. In the formamide ethyl derivative complexes, for both monodentate and bidentate bindings, the **g** rotamer was the lowest in energy. In the ethyl derivatives of the tautomer isomers, the **a** rotamer is the most stable of the rotamers.

Overall the effect of complexation on these ligands is similar to those found in the earlier cases. The monodentate X−O bond length is longer than that found in the previous sections. It is also remarkable that the Al−ligand bond lengths are the largest in this series (excluding the **E-Aln2.3a** and **E-Aln2.4a** complexes); however, the corresponding bond lengths of the magnesium complexes are the shortest (with the exception of **E-Mgn2.3a** and **E-Mgn2.4a** complexes). In the **E-Aln2.3a** and **E-Aln2.4a** complexes, due to the interactions between aluminum and the terminal carbon, which lead to a formation of a ring, the Al−N bond lengths are the shortest found with lengths of 1.785 and 1.797 Å, respectively.

The binding energies of these ethyl complexes in comparison to those of the methyl set present significant changes for the aluminum(III) complexes, yet remain similar for the magnesium(II) complexes. Due to the aluminum interactions with the terminal carbon in rotamers **Al-n2.3a** and **Al-n2.4a** (depicted in Figure 2), the binding energies of these complexes are the strongest found in this study with a value of 404 kcal/mol in both complexes. **Al-b2.2b** and **Al-n2.1e** complexes have binding energies of 393 and 382 kcal/mol, respectively. Finally the binding energies of the ethylformamide derivatives are 390 and 377 kcal/mol for **Al-o1c** and **Al-bts1f**, respectively. For the magnesium complexes, a tendency similar to that found in the previous formamide and methyl derivatives is observed, where the binding energies range from 145 kcal/mol in **Mg-o1g** and **Mg-b2.2a** to 125 kcal/mol in **Mg-bts1g** and **Mg-n2.1a**.

In terms of the natural charge distribution, it can be observed in Table 5 that these ethyl complexes allow the largest charge transfer from the ligand to the cation; e.g., the lowest aluminum positive charge was found in the **E-Aln2.1e** complex (1.791 e^-), and for magnesium in complex **E-Mgbts1g** (1.833 e^-). This effect was also observed for the acidic amino acid chains.[10] Upon the addition of a methyl group to formamide, the bidentate bonding complexes were preferentially stabilized. However, in the aluminum complexes, when that methyl is replaced with an ethyl group, the monodentate complexes are preferentially stabilized. (Note that we are comparing the bidentate complexes with the monodentate complexes, which do not have direct interactions with the terminal carbon.) Though, the difference in charge transfer to aluminum upon changing Y from CH_3 to CH_2CH_3 shows no clear pattern of difference between mono- and bidentate cases.

Turning to the Bader analysis, as seen previously, the atom binding to the metal cation experiences a positive energy density shift in its bond to carbon, while the bond between carbon and the other atom shifts negatively. The Al−C bonds appearing in the **E-Aln2.3a** and **E-Aln2.4a** complexes are reported to be covalent bonds, and a ring critical point is also located. To get better descriptions of these bonds, NBO analysis was performed for these complexes, and no 3c,2e bond was reported, but a strong second-order interaction from the out-of-plane σ C−H bonds to the aluminum empty p orbital (around 18 kcal/mol in both structures) and from the same C−H bonds to the σ^* Al−N (around 4 kcal/mol in both structures) was found. Note that, in these two complexes, we lose the free rotor character of the ethyl group, since there is no other rotamer stationary point on the **E-Aln2.4** surface, and the only additional stationary point located for **E-Aln2.3** is the rotamer **d**, which is a transition state 33 kcal/mol higher in energy.

IV. Conclusions

We have studied the interactions between the asparagine and glutamine amino acid chains with aluminum(III) and magnesium(II) cations in the gas phase. We started with the formamide and one of its tautomers, which is the smallest functional group in both amino acids and the simplest prototype that contains

the peptide linkage. We have added a methyl group to represent more accurately the asparagine, and an ethyl group for the glutamine. These end groups, in general, were found to be more or less free rotors, and due to this fact, there are many binding and rotamer possibilities. The free rotor character is lost in some complexes after the interactions between the aluminum and the terminal carbon residue. Cartesian coordinates, frequencies, and energies for all stationary points located are available upon request.

We have also observed the importance of the formamide tautomer derivative−metal cation interactions since the strongest binding occurs with the tautomer. Over the different basic centers of the formamide, the bidentate binding with complex **2.2** is favored over monodentate Al−O or Al−N binding in all cases except in the **E**-formamide derivatives **n**, in which the Al−N binding in **Aln2.3** and **Aln2.4** is preferred due to the Al−C interactions. For magnesium, similarly, the bidentate bonding with the tautomer is the strongest in the whole series. However, note the difference in binding energy between the complexes in which magnesium(II) is bound in a bidentate manner to the tautomers and the **Mgo1**, **M-Mgo1**, **E-Mgo1** complexes is very small.

The inclusion of the methyl and ethyl groups to simulate the asparagine and glutamine amino acid chains was also found to be important. Significant differences in binding energy were found upon the addition of the methyl group, and while the energetic effect of changing the methyl for an ethyl was smaller, it was still important for both cations studied and larger in the case of aluminum bonding. Also the increase in charge transfer to the metal center increased as the size of Y increased (again this was especially noticeable in the case of aluminum). What is more, the interactions between the complexing aluminum atom but not the magnesium atom with the terminal carbon atom in two of the $Y = CH_2CH_3$ cases demonstrate another manner in which aluminum may have a competitive advantage over magnesium in binding to biologically important ligands.

The binding of asparagine and glutamine chains studied here to the cations under investigation is weaker than binding of aspartic acid and glutamic acid amino acid chains to these same cations.[10]

Acknowledgment. J.M.M. and J.E.F. thank the Basque Government (Eusko Jaurlaritza) for a grant. Financial support from the Spanish DGICYT (Grant No. PB96/1524) and from the Provincial Government of Gipuzkoa (Gipuzkoako Foru Aldundia) is gratefully acknowledged.

References and Notes

(1) Williams, R. J. P. *Coord. Chem. Rev.* **1996**, *149*, 1.
(2) Pohlmeier, A.; Knoche, W. *Int. J. Chem. Kinet.* **1996**, *28*, 125−136.
(3) Candy, J. M.; McArthur, F. K.; Oakley, A. E.; Taylor, G. A.; Mountfort, C. P. L.; Thompson, J. E.; Chalker, P. R.; Bishop, H. E.; Beyreuther, K.; Perry, G.; Ward, M. K.; Martin, C. N.; Edwardson, J. A. *J. Neurol. Sci.* **1992**, *107*, 210−218.
(4) Meri, H.; Banin, E.; Roll, M.; Rousseau, A. *Prog. Neurobiol.* **1993**, *40*, 89−121.
(5) Bhattacharyya, M. H.; Wilson, A. K.; Silbergeld, E. K.; Watson, L.; Moreti, S.; et al. In *Metal Toxicology*; Goyer, R. A.; Klaassen, C. D.; Waalkes, M. P., Eds.; Academic Press: San Diego, 1995; p 525.
(6) Armstrong, R. A.; Winsper, S. J.; Blair, J. A. *Dementia* **1996**, *7*, 1−9.
(7) Macdonald, T. L.; Martin, R. B. *Trends Biochem. Sci.* **1988**, *13*, 15−19.
(8) Martin, R. B. *Clin. Chem.* **1986**, *32*, 1797.
(9) Ganrot, P. O. *Environ. Health Period.* **1986**, *65*, 363.
(10) Mercero, J. M.; Fowler, J. E.; Ugalde, J. M. *J. Phys. Chem.* **1998**, *102* (35), 7006−7012.
(11) Garmer, D. R.; Gresh, N. *J. Am. Chem. Soc.* **1994**, *116*, 3556−3567.
(12) Gresh, N.; Stevens, W. J.; Krauss, M. *J. Comput. Chem.* **1995**, *16*, 843−855.
(13) Gresh, N.; Garmer, D. R. *J. Comput. Chem.* **1996**, *17*, 1481−1495.
(14) Deerfield, D. W.; Fox, D. J.; Head-Gordon, M.; Hiskey, R. G.; Pedersen, L. G. *Proteins* **1995**, *21*, 244−255.
(15) Perrin, C. I. *Acc. Chem. Res.* **1989**, *22*, 286.
(16) Antonczack, S.; Rouiz-Lopez, M.; Rivail, J. *J. Am. Chem. Soc.* **1994**, *116* (9), 3912−3921.
(17) Tortajada, J.; Leon, E.; Morizur, J.-P.; Luna, A.; Mo, O.; Yanez, M. *J. Phys. Chem.* **1995**, *99*, 13890−13898.
(18) Tortajada, J.; Leon, E.; Luna, A.; Mo, O.; Yanez, M. *J. Phys. Chem.* **1994**, *98*, 12919−12926.
(19) Luna, A.; Amekraz, B.; Tortajada, J.; Morizur, J. P.; Alcami, M.; Mo, O.; Yanez, M. *J. Am. Chem. Soc.* **1998**, *120*, 5411−5426.
(20) Kiss, T.; Sovago, I.; Toth, I.; Lakatos, A.; Bertani, R.; Tapparo, A.; Bombi, G.; Martin, R. B. *J. Chem. Soc., Dalton Trans.* **1997**, 1967−1972.
(21) Bottari, E.; Festa, M. R. *Ann. Chim.* **1996**, *86*, 133−142.
(22) Schröder, D.; Schwarz, H. *J. Phys. Chem. A* **1999**, *103*, 7385.
(23) GAUSSIAN 98, Rev. A.5: Frisch, M. J.; Trucks, G. W.; Schlegel, H. B.; Scuseria, G. E.; Robb, M. A.; Cheeseman, J. R.; Zakrzewski, V. G.; Montgomery, J. A.; Stratmann, R. E.; Burant, J. C.; Dapprich, S.; Millam, J. M.; Daniels, A. D.; Kudin, K. N.; Strain, M. C.; Farkas, O.; Tomasi, J.; Barone, V.; Cossi, M.; Cammi, R.; Mennucci, B.; Pomelli, C.; Adamo, C.; Clifford, S.; Ochterski, J.; Petersson, G. A.; Ayala, P. Y.; Cui, Q.; Morokuma, K.; Malick, D. K.; Rabuck, A. D.; Raghavachari, K.; Foresman, J. B.; Cioslowski, J.; Ortiz, J. V.; Stefanov, B. B.; Liu, G.; Liashenko, A.; Piskorz, P.; Komaromi, I.; Gomperts, R.; Martin, R. L.; Fox, D. J.; Keith, T.; Al-Laham, M. A.; Peng, C. Y.; Nanayakkara, A.; Gonzalez, C.; Challacombe, M.; Gill, P. M. W.; Johnson, B. G.; Chen, W.; Wong, M. W.; Andres, J. L.; Head-Gordon, M.; Replogle, E. S.; Pople, J. A., Gaussian, Inc., Pittsburgh, PA, 1998.
(24) Labanowsky, J.; Andelzelm, J. *Density Functional Methods in Chemistry*; Springer-Verlag: New York, 1991.
(25) Tschinke, V.; Ziegler, T. *Theor. Chim. Acta* **1991**, *81*, 651.
(26) Johnson, B. G.; Gill, P. M. W.; Pople, J. A. *J. Chem. Phys.* **1993**, *98*, 5612.
(27) Becke, A. D. *J. Chem. Phys.* **1993**, *98*, 5648.
(28) Lee, C.; Yang, W.; Parr, R. G. *Phys. Rev. B.* **1988**, *37*, 785.
(29) Stevens, W. J.; Krauss, M.; Basch, H.; Jasien, P. G. *Can. J. Chem.* **1992**, *70*, 612.
(30) Bader, R. F. W. *Atoms in Molecules: A Quantum Theory*; Clarendon Press, Science Publications: Oxford, 1990; Chapter 7.
(31) Biegler-Koning, F. W.; Bader, R. F. W.; Tang, T. H. *J. Comput. Chem.* **1980**, *27*, 1924.
(32) NBO version 3.1: Glendening, E. D.; Reed, A. E.; Carpenter, J. E.; Weinhold, F.
(33) Molden: http://www.caos.kun.nl/~schaft/molden/molden.html.
(34) Francl, M. M.; Pietro, W. J.; Hehre, W. J.; Binkley, J. S.; Gordon, M. S.; DeFrees, D. J.; Pople, J. A. *J. Chem. Phys.* **1982**, *77*, 3654.